An Acad Bras Cienc (2024) 96(Suppl. 1): e20230423 DOI 10.1590/0001-3765202420230423
Anais da Academia Brasileira de Ciências | *Annals of the Brazilian Academy of Sciences*
Printed ISSN 0001-3765 I Online ISSN 1678-2690
www.scielo.br/aabc | www.fb.com/aabcjournal

CHEMICAL SCIENCES

Biological evaluation of benzothiazoles obtained by microwave-green synthesis

MESUT OZDINCER, ASLIHAN DALMAZ, SEFA DURMUS, GORKEM DULGER & ILKER KILICCIOGLU

Abstract: Benzothiazole compounds are known as an important bicyclic ring system with multiple applications. These compounds have a wide range of biological activities, including anticancer, antimicrobial, anti-inflammatory and antiviral activities. In this study, benzothiazole compounds were synthesized and their various biological activities were examined. The synthesized benzothiazoles were evaluated for their antimicrobial properties against various bacterial and fungal strains. The compound **6e** is most active ligand in the series against bacteria and fungi as compared to standard antibiotics. Especially, this compound significant effect against *Staphylococcus aureus* (32.00 ± 1.73 mm). These compounds exhibited potent anticancer activity against gastrointestinal cancer cells, demonstrating their potential as therapeutic agents. The lowest antiproliferative response after administration of the compounds was observed in HCT116 cells, while the most effective antiproliferative response was observed in AGS cells (> 10 µg/mL). In all cell lines, 40 and 100 µg/mL application values of the selected compounds showed significant increases in the expression of caspase-3, 8 and 9. We also utilized a computational docking approach to investigate the interaction of these benzothiazoles with VEGFR-2 kinase. Our docking studies showed that compounds **6a** and **6d** may be promising therapeutic agents against gastrointestinal system cancers due to their ability to bind to VEGFR-2 kinase.

Key words: Benzothiazole, Molecular evolution, Docking studies, Antimicrobial, Antiproliferative, Gastrointestinal cancer cells.

INTRODUCTION

Research on heterocyclic ligands, which consist of electron-rich atoms such as sulfur, nitrogen and oxygen is constantly increasing due to their wide range of potential applications. Specifically, among these compounds, disulfides (Flores-Álvarez et al. 2022, Yao et al. 2022, Shi et al. 2022), thio compounds (Dalmaz et al. 2021, 2022, Kannaiyan et al. 2022), disulfide-containing Schiff bases (Bhowon et al. 2021, Durmus et al. 2017, Asadizadeh et al. 2022), thiophenes (Sivrikaya et al. 2018) and hydroxy-substituted benzothiazoles (Shainyan et al. 2022, Amalraj et al. 2022, Kumar & Singh 2021), have featured prominently. Their strong pharmacological effects and ability to form unique chemical structures explain the importance of these compounds. Benzothiazoles represent an important class of heterocyclic compounds, having a wide range of applications (Abd El-Meguid et al. 2022, Hsu & Ding 2022). In addition to their industrial applications as antioxidants (Racané et al. 2020), vulcanization accelerators (Morgan & McGill 2000) and corrosion inhibitors (Xu et al. 2016), these compounds are used in the development of sensor molecules (Stenger-Smith et al. 2018) as they can exhibit properties such as nonlinear optical properties

(Ghanavatkar et al. 2019, Shivani et al. 2020) and luminescence/fluorescence (Azzam et al. 2020), which makes them particularly important.

The benzothiazole core is an important drug-like scaffold that has been used as a precursor for the design and discovery of potent agents such as antimicrobial (Mohamed et al. 2021, Ghannam et al. 2019, Fadda et al. 2019), antifungal (Luo et al. 2018, Sirgamalla et al. 2020), anti-inflammatory (Shafi et al. 2012), antituberculosis (Cordeiro & Kachroo 2020) and anti-cancer (Uremis et al. 2017, Irfan et al. 2020, Dhadda et al. 2021, El-Meguid et al. 2022). Most medicines used for treatment act as antimicrobials, which are designed to inhibit the growth and reproduction of bacteria. However, misuse can lead to the increasing prevalence of antibiotic-resistant diseases. Despite significant advances in antimicrobial therapy, infectious diseases caused by bacteria or fungi still pose a significant threat (Aslam et al. 2018). Mohamed et al. (2021) synthesized benzothiazole derivatives and evaluated their antibacterial activity against both Gram-positive and Gram-negative bacteria. All compounds showed excellent antibacterial activity. In another study, Malah et al. (2022) synthesized new benzothiazole-1,2,3-triazole compounds via CuAAC reaction with substituted azide derivatives of alkyne-functionalized benzothiazole. They performed in vitro antimicrobial experiments to evaluate the activity of these new compounds against *B. cereus, S. aureus, E. coli, P. aeruginosa, F. solani,* and *C. albicans*. The findings indicated that the novel derivatives showed increased effectiveness against Gram-negative bacteria while displaying lower activity against Gram-positive bacteria. They predicted that this different activity could be attributed to the difference in cell wall composition between the two species (Malah et al. 2022).

Cancer is the second leading cause of mortality in the world. Cancer is a very complex health problem that is an important research topic in today's medical science. The development of drugs and procedures for safer and more effective treatment is important in the medical scientific community (Debela et al. 2021). Neoplastic tumor cells are heterogeneous cells capable of rapid proliferation. These neoplasm malignant tumors have the potential to spread through the bloodstream and lymphatic system to other parts of the body through a process called metastasis. This situation creates a major obstacle to treatment (Azzam et al. 2022, Anand et al. 2008). Cancers originating from the gastrointestinal tract, including the esophagus, stomach, colorectum, liver and pancreas are a major health problem, one of the leading causes of cancer-related deaths worldwide (Bray et al. 2018). The traditional treatment strategy for gastrointestinal cancers is surgical resection. However, unresectable or recurrent patients are treated with palliative chemotherapy or radiotherapy.

It is ongoing research to develop chemotherapeutic agents with reduced drug exposure, fewer side effects and stronger antitumor efficacy *in vitro* and *in vivo*. These studies are important for treating patients who do not respond to treatment or who develop resistance to chemotherapy (Gediya & Vincent 2009, Marco-Contelles & Soriano 2011).

One of the most important ways in cancer treatment is to control the uncontrolled growth of cancer cells. Targeting apoptosis using molecular mechanisms for cancer cell death is a successful and effective non-surgical treatment (Pfeffer & Singh 2018). Apoptosis is executed by initiator and executioner caspase proteins (cysteine aspartyl-specific proteases) which are a class of cysteine proteins that cleave target proteins. The caspases, namely caspase-3,

caspase-8, and caspase-9, are enzymes of significant importance in programmed cell death and hold critical roles in cancer. Caspase-3, also referred to as the "executioner caspase," becomes activated upon exposure to various apoptotic signals and is indispensable for carrying out the apoptotic process. Caspase-8, an initiator caspase, is triggered by death receptors, and its activation subsequently leads to the activation of downstream caspases, including caspase-3. Caspase-9, another initiator caspase, is activated by the release of cytochrome c from the mitochondria and plays a pivotal role in the intrinsic pathway of apoptosis. These caspases have been identified as potential targets for cancer therapy (Boice & Bouchier-Hayes 2020, Opdenbosch & Lamkanf 2019). Apoptosis occurs in two ways being. The intrinsic pathway which is driven by the BCL-2 (B-cell lymphoma-2) family, which includes proapoptotic proteins and is activated by mitochondrial proteins or via an extrinsic pathway, which uses extracellular signals and is activated by the activation of death receptors on the cell surface (Zaman et al. 2014, Xu et al. 2015). Loss of apoptotic control allows cancer cells to survive longer, as well as promotes invasion, angiogenesis, and accumulation of mutations during tumor progression. For these reasons, there is a need for selective agents that can induce apoptosis of tumor cells.

In recent years, the synthesis of substituted benzothiazoles has garnered considerable attention owing to their extensive range of applications. This has led to a surge in research dedicated to this area. Several synthetic methods have been reported for the production of benzothiazoles (Dhawale et al. 2021, Nguyen et al. 2019, Gao et el. 2020, Wagay et al. 2022, Yu et al. 2020, Bouchet et al. 2020, Maity et al. 2021, Kazi & Sekar 2019, Sedaghat et al. 2014). Microwave-assisted synthesis is widely used for the efficient synthesis of heterocyclic compounds (Rapolu et al. 2019, Patel et al. 2021, Das & Banik 2021). Utilizing microwave irradiation in organic synthesis aligns with the principles of green chemistry by minimizing solvent usage, decreasing side reactions, and enhancing purity, efficiency and energy utilization. In this context, in our study, the reaction of 2-amino thiophenol and aromatic aldehydes was carried out using microwave irradiation and under an argon atmosphere. In this reaction, hydroxyphenyl benzothiazoles were obtained without any by-products forming as a result of the reaction. By comparison with the reported same articles shows that the most effective method is to use of microwave irradiation. In addition, the structures of all synthesized bioactive heterocyclic compounds were elucidated using spectroscopic methods such as fourier transform infrared (FT-IR), nuclear magnetic resonance (^{1}H-NMR, ^{13}C-NMR) and ultraviolet-visible (UV-Vis) spectroscopy. It was decided to perform a thermogravimetric analysis (TGA) in order to examine the thermal stability of mentioned compounds and their plausible degradation. In this study, the in vitro antimicrobial activity of ligands against various strains and yeasts was also evaluated by the well diffusion technique. In addition, the antiproliferative effects of the compounds were investigated in AGS (gastric cancer), HepG2 (hepatocellular carcinoma) and HCT116 (colorectal cancer) cell lines. To the best of our knowledge, our study was the first to be studied not on a single cell line from the gastrointestinal cancer group, but on three cell lines, namely colon, liver and stomach cancer cell lines. In addition, caspase-3, 8 and 9 expression changes in these cells as a result of treatment with the compounds were evaluated. Finally, the effect of selected compounds on the migration levels of cells in AGS cells that gave the best antiproliferative response to the

compounds was also examined. A molecular docking study was conducted to examine the binding affinity of the most potent derivatives on VEGFR-2 active sites.

EXPERIMENTAL

Reagents and apparatus

All chemicals in the study were provided commercially. No purification process was applied. 2-aminothiophenol, 2-hydroxy benzaldehyde, 3-hydroxy benzaldehyde, 4-hydroxybenzaldehyde, 2,3-dihydroxy benzaldehyde, 2,4 dihydroxy benzaldehyde, 3,4-dihydroxy benzaldehyde, methanol, dichloromethane and ethanol were purchased from Merck. Melting points were measured using Stuart Equipment. FT-IR spectroscopy results were recorded using a Shimadzu IR Prestige FT-IR Spectrophotometer coupled with the ATR apparatus. ^{1}H-NMR studies were performed with a 400 MHz Bruker Avance NMR Spectrometer. ^{13}C-NMR spectra were recorded using DMSO-d_6 solvent on a Bruker spectrometer operating at 101 MHz. DMSO-d_6 was used as the solvent for all compounds and chemical shifts were reported in ppm from the internal reference $(CH_3)_4Si$. TGA-differential thermal analysis (DTA) curves were obtained using a Shimadzu DTG-60H instrument with a flow rate of 100 mL min^{-1} under nitrogen atmosphere. The heating rate was 10 °C/min. UV absorption and fluorescence emission studies were performed at ambient temperature, using CH_2Cl_2 solvent with PG Instruments T80 dual beam spectrophotometer and Shimadzu RF 5301PC Fluorescent Spectrophotometer, respectively.

General procedure of synthesis compounds

(Method A) Benzothiazoles (**6a**-**f**) were synthesized by mixing commercially available 2-aminothiophenol (10 mmol) and hydroxy aromatic aldehydes (10 mmol) in ethanol. At room temperature, the reaction mixtures were carried out under an argon atmosphere. The product formation process for all reactions was followed by thin layer chromatography. After the formation of the product, it was filtered and recrystallized with methanol to obtain the formed products in a purer form.

(Method B) Benzothiazoles (**6a**-**f**) were synthesized by mixing commercially available 2-aminothiophenol (10 mmol) and hydroxy aromatic aldehydes (10 mmol) in ethanol and irradiated in a microwave oven. In order to advance the experimental process in a controlled manner, the reaction mixture was cooled to room temperature conditions every minute and the resulting change was observed. It was determined that the product formation process was completed by thin layer chromatography and the reaction mixture was filtered. It was recrystallized using a methanol/dichloromethane mixture to obtain pure products of the reaction.

2-(2-hydroxyphenyl)benzothiazole (6a): pale yellow solid, mp 136 °C (Khan et al. 2011, Das et al. 2012). UV-Vis spectrum (CH_2Cl_2, nm) λ_{max}: 227 and 317 nm. IR spectrum, ν, cm^{-1}: 3150 (O-H), 1587 (C=N), 1485 (C=C), 1219 (C-O), 748 (C-S). ^{1}H-NMR spectrum, δ, ppm (*J*, Hz): 12.56 (s, 1H, OH); 7.98 (d, *J* = 8.0, 1H, N=$CH_{(thiazole)}$), 7.88 (d, *J*= 8.0, 1H, Ar-H), 7.70–7.67 (m, 1H, Ar-H), 7.51–7.47 (m, 1H, Ar-H), 7.41–7.37 (m, 2H, Ar-H), 7.10 (d, *J* = 8.0, 1H, Ar-H), 6.95 (t, *J* = 7.6, 1H, Ar-H). ^{13}C-NMR spectrum, δ, ppm: 169.6; 158.2; 152.1; 137.7; 132.9; 130.4; 128.6; 126.9; 125.7; 122.4; 121.7; 119.7; 118.1.

2-(3-hydroxyphenyl)benzothiazole (6b): white solid, mp 132 °C. UV-Vis spectrum (CH_2Cl_2, nm) λ_{max}: 227 and 313 nm. IR spectrum, ν, cm^{-1}: 3059 (O-H), 1597 (C=N), 1435 (C=C), 1265 (C-O), 739 (C-S). ^{1}H-NMR spectrum, δ, ppm (*J*, Hz): 9.92 (s, 1H, OH), 8.13 (d, *J* = 8.0, 1H, N=$CH_{(thiazole)}$), 8.06 (d, *J* = 8.0, 1H, Ar-H), 7.57-7.51 (m, 3H, Ar-H), 7.46 (t, *J* =7.6,

1H, Ar-H), 7.37 (t, *J* =8.0, 1H, Ar-H), 6.99 (d, *J* =8.0, 1H, Ar-H); ^{13}C-NMR spectrum, δ, ppm: 167.8; 158.5; 154.0; 135.0; 134.5; 131.1; 127.1; 126.0; 123.3; 122.7; 119.0; 118.6; 113.9.

2-(4-Hydroxyphenyl)benzothiazole (6c): white solid, mp 231 °C [54]. UV-Vis spectrum (CH_2Cl_2, nm) λ_{max}: 224 and 310 nm. IR spectrum, v, cm^{-1}: 3010 (O-H), 1602 (C=N), 1427 (C=C), 1282 (C-O), 738 (C-S). ^{1}H-NMR spectrum, δ, ppm (*J*, Hz): 9.94 (s, 1H, OH), 8.06 (d, *J* = 8.0, 1H, N=$CH_{(thiazole)}$), 7.99 (d, *J* = 8.8, 2H, Ar-H), 7.91 (d, *J* = 8.0, 1H, Ar-H), 7.50 (t, *J* = 8.0, 1H, Ar-H), 7.39(t, *J* = 8.0, 1H, Ar-H), 6.95 (d, *J* = 8.8, 2H Ar-H). ^{13}C-NMR spectrum, δ, ppm: 167.9; 160.8; 154.0; 134.4; 129.3 (2C); 126.8; 125.2; 124.3; 122.6; 122.4; 116.4 (2C).

2-(2,3-Dihydroxyphenyl)benzothiazole (6d): light brown solid, mp 186 °C. UV-Vis spectrum (CH_2Cl_2, nm) λ_{max}: 225 and 321 nm. IR spectrum, v, cm^{-1}: 3489 (O-H), 1597 (C=N), 1469 (C=C), 1274 (C-O), 752 (C-S). ^{1}H NMR spectrum, δ, ppm (*J*, Hz): 8.13 (d, *J*=8.4 ,1H), 7.56-7.53 (m, 2H), 7.44 (t, *J*= 6.8 Hz, 1H), 6.96 (d, *J*=7.6 Hz, 1H), 6.85-6.81 (m, 1H). ^{13}C-NMR spectrum, δ, ppm: 166.9; 151.8; 146.7; 146.1; 134.3; 127.1; 125.7; 122.5; 122.4; 120.0; 118.7; 118.2; 118.0.

2-(2,4-Dihydroxyphenyl)benzothiazole (6e): yellow solid, mp 143 °C. UV-Vis spectrum (CH_2Cl_2, nm) λ_{max}: 225 and 311 nm; IR spectrum, v, cm^{-1}: 3441 (O-H), 1598 (C=N), 1475 (C=C), 1217 (C-O), 751 (C-S). ^{1}H-NMR spectrum, δ, ppm (*J*, Hz): 11.68 (s, 1H, OH), 10.19 (s, 1H, OH), 8.09 (d, *J* = 8.0, 1H, N=$CH_{(thiazole)}$), 7.97 (d, *J* = 8.4, 1H, Ar-H), 7.93 (d, *J* = 9.6, 1H, Ar-H), 7.50 (t, *J* = 8.0, 1H, Ar-H), 7.39 (t, *J* = 8.0, 1H, Ar-H), 6.48-6.46 (m, 2H, Ar-H). ^{13}C-NMR spectrum, δ, ppm: 162.1; 158.7; 151.9; 133.7; 130.5; 126.8; 125.3; 124.0; 122.3; 121.8; 110.6; 108.9; 103.1.

2-(3,4-Dihydroxyphenyl)benzothiazole (6f): pale yellow solid, mp 223 °C. UV-Vis spectrum (CH_2Cl_2, nm) λ_{max}: 226 and 307 nm. IR spectrum, v, cm^{-1}: 3059 (O-H), 1597 (C=N), 1435 (C=C), 1265 (C-O), 739 (C-S). ^{1}H-NMR spectrum, δ, ppm (*J*, Hz): 9.6 (s, 2H, OH), 8.06 (d, *J* = 8.0, 1H, N=$CH_{(thiazole)}$), 7.97 (d, J = 8.4, 1H, Ar-H), 7.52 (d, *J* = 8.4, 1H, Ar-H), 7.48 (t, *J* = 8.0, 1H, Ar-H), 7.41-7.37 (m, 2H, Ar-H), 6.90 (d, *J* = 8.4, 1H, Ar-H); ^{13}C-NMR spectrum, δ, ppm: 168.1; 154.2; 149.5; 146.3; 134.6; 126.9; 125.3; 124.8; 122.7; 122.5; 119.9; 116.6; 114.5.

Molecular docking studies

Molecular docking studies have been carried out to examine the interaction of the synthesized compounds with vascular endothelial growth factor receptor-2 (VEGFR-2). For the evaluation of anti-cancer mechanisms, the crystalline structures of target protein (PDB ID: 2XIR) (Matsunaga et al. 2005) were obtained from the protein data bank (https://www.rcsb.org). The synthesized derivatives were drawn using ChemDraw 19.1 software and energy minimized with Chem3D 19.1 software and saved in (.pdb) format for docking evaluation. Molecular docking studies were performed by using the Autodock tools (ADT) v.1.5.7 (MGL tools 1.5.7) (Allouche 2010) by interacting with the synthesized compounds (**6a**-**6f**) with the 2XIR target enzyme. The active site of the target protein was defined by placing a suitable grid box around the co-crystal ligand. The grid box had dimensions of X: 98, Y: 86, Z: 72 Å and a grid spacing of 0.449 Å, with its center located at X: 3.487, Y: 36.079, Z: 15.877. As a result of molecular docking studies, the interactions of **6a** and **6d** compounds against target enzyme with the best affinity score were investigated. Discovery Visualizer Software copyright 2021 Client (Biovia) was used to visualize and analyze target protein-ligand interactions.

Antimicrobial Screening

Test Microorganisms

The *in vitro* antimicrobial studies were carried out with four bacteria strains (*Escherichia coli*, *Staphylococcus aureus*, *Pseudomonas aeruginosa* and *Enterococcus faecalis*) and

three yeast strains (*Candida albicans*, *Candida parapsilosis* and *Candida krusei*) obtained from Duzce University Medical Biology Laboratory.

Well Diffusion Method

Well diffusion method was used to determine antibacterial and antifungal activity of benzothiazole compounds (**6a-6f**). Nutrient Broth was used for bacteria and Malt Extract Broth was used for fungi to prepare 24 hour young cultures of microorganisms. After preparation according to 0.5 McFarland standardization, bacteria were incubated at 35-37 °C and fungi at 25-27 °C for 24-48 hours. In order to compare the antimicrobial activity of levels of benzothiazole compounds (**6a-6f;** 30 µg/mL), Ampicillin, Amikacin (BIOANALYSE) antibiotics were used for bacteria, while Nystatin (BIOANALYSE) antibiotic was used for fungi. The compound's antimicrobial activity experiments were performed in triplicate.

Antiproliferative Evaluation

Cell culture

HCT116 (colon cancer cell line, ATCC Number: CCL-247), AGS (gastric cancer cell line, ATCC Number: CRL-1739) and HepG2 (hepatocellular carcinoma cell line, ATCC Number: HB-8065) cell lines were used in this study. Cells were grown in RPMI-1640 and DMEM media supplemented with 10% inactivated Fetal Bovine Serum, (FBS), 200 mM L-glutamine, 100 µ/mL penicillin, 100 pg/mL streptomycin. They were cultured in the incubator (Nuve, Türkiye) at 5% CO_2 and 37 °C. Cells were grown in a 75 cm^2 flask until they reached a density of about 80%. The culture medium was changed once every 48 h.

Cell Proliferation Assay (WST-1 method)

The media was removed when the HCT116, AGS, HepG2 cell lines reached approximately 70-80% confluency in T-75 cell flasks. Cells were separated from the base and each other using trypsin-EDTA mixture. After centrifugation at 1200 rpm for 10 minutes, RPMI-1640/DMEM medium containing 1% FBS was added to the pellet. Then, cells were homogeneously suspended in RPMI-1640/DMEM medium containing 1% FBS, and then seeded into 96-well cell culture dishes by drawing approximately 5000 cells/100 µL into each well. After the cells were incubated overnight in incubator at 37 °C and 5% CO_2, the media were removed. The series of synthesized benzothiazole compounds **(6a-6f)** at the specified concentrations (5-100 µg/mL) were added to the cells and incubated in a medium containing 1% FBS for 24 hours at 37 °C with 5% CO_2. At the end of the specified time, the medium in each well was removed and replaced with 100 µL of phenol-red-free RPMI-1640/DMEM medium and 10 µL of WST-1 kit. The color change caused by the formazan product was determined at the wavelength range of 450 nm with a microplate reader (Epoch Microplate Spectrophotometer, Agilent Technologies, Inc., USA) after 4 hours. Each experiment was performed in triplicate. Cell viability calculations were made on the Excel program.

Protein isolation and ELISA assay

Protein isolation was performed 24 hours after the application of selected compounds to HCT116, AGS, HepG2 cells at concentrations of 40 and 100 µg/mL, with RIPA buffer (A.B.T, Türkiye) following the appropriate protocol steps. BCA protein assay kit (ABP Biosciences, LLC) was used to determine the amount and concentration after protein isolation.

Colorimetric human Caspase-3, 8 and 9 ELISA kits (BT LAB, Shanghai, China) were used to determine protein expression levels of Caspase-3, 8 and 9 in cell supernatant samples treated with compounds according to manufacturer's instructions. After the procedures, the results

were obtained by reading the ELISA reader (Epoch Microplate Spectrophotometer, Agilent Technologies, Inc., USA) at Optical Density (OD) at 450 nm.

Wound healing assay

AGS cells were grown on a 6-well plate until they reached at least 90% confluency in DMEM medium. Plate scraping was performed using a 100 µL pipette tip when cells were treated with the selected compounds. Cells were incubated in three groups as control group, 24 and 48 hours. Images were acquired for AGS cells under an inverted microscope (Euromex, Arnhem, The Netherlands) at 0, 24 and 48 hours.

Statistical analysis

Each experiment was performed in triplicate independently of each other. Excel program was used to evaluate the cell viability data. All experiments were carried out in triplicate independently of each other. The data of the experiments were statistically analyzed using One sample t-test. Values with $p < 0.05$ were considered significant.

RESULT AND DISCUSSION

Chemistry

We report here, the synthesis of hydroxy phenyl benzothiazole as the only product by heating the reaction of 2-aminothiophenol with aromatic aldehydes both through microwave irradiation and under argon atmosphere. In our research, we developed a method suitable for the synthesis of 2-substituted benzothiazole analogs in green conditions. Comparative aspects in terms of yield and reaction rate are shown in Table I, which compares reaction time and product yield for the conventional and microwave methods. The microwave method was found to be better than the conventional method as there was a significant reduction in the reaction rate.

Microwave is superior in terms of reaction rate with a reduction of about 25 times and an increase in product yield of 12 to 20%. For the development of microwave assisted synthesis of benzothiazole derivatives, Zhang et al. synthesized benzothiazole derivatives in microwave using glycerol as solvent. Compared to our study, we found more favorable results both in terms of yield because of the potential of solvent such as glycerin to cause side reactions and in terms of reaction time (Zhang et al. 2012). The green synthesis of benzothiazoles was performed using the microwave irradiation method, which has the advantage of being highly efficient, environmentally friendly less time-consuming and energy efficient as well as being extremely efficient. We also studied that all synthesized bioactive heterocycles compounds carried by FT-IR, ^{1}H-NMR, ^{13}C-NMR and UV-Vis.

An electron pair of the amino group is attacked on the carbonyl group of aldehydes by heating or irradiation one molecule of water leave structure to give Schiff bases then an electron pair of sulfur atoms is attacked on the imine group, cyclize spontaneously to give the corresponding benzothiazoline. These compounds are then oxidized by air to give benzothiazoles. The intramolecular cyclization reaction consists of Schiff base formation.

In this study, hydroxy-substituted phenyl benzothiazoles were synthesized using two different methods, argon atmosphere and microwave irradiation. The structures of the obtained ligands are given in Table I. The spectral results of the synthesized ligands were compared with the literature data (Khan et al. 2011, Das et al. 2012).

Table I. Structures of synthesized hydroxy substituted phenyl benzothiazoles compounds and reaction parameters 6a-6f.

Aldehyde		Product[a]		Time		Yield (%)[b]	
				Method A (h.)	Method B (min.)	Method A	Method B
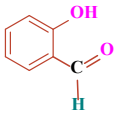	(2a)	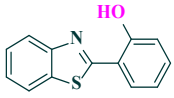	(6a)	4	8	70	92
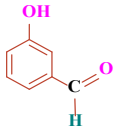	(2b)	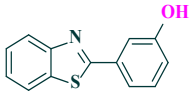	(6b)	6	8	72	85
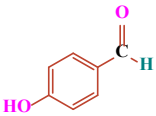	(2c)	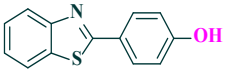	(6c)	2	6	68	90
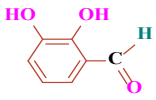	(2d)	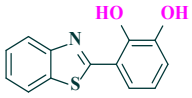	(6d)	10	8	45	75
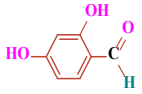	(2e)	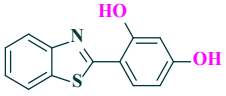	(6e)	6	8	52	85
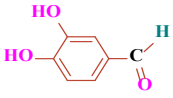	(2f)	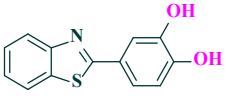	(6f)	6	8	72	90

[a]Solvent: EtOH; [b]All compounds **6a-6f** were isolated.

Characterization of Benzothiazoles

FT-IR spectral studies

The structures of **6a-6f** were confirmed by FT-IR spectroscopy. When the FT-IR spectra of the synthesized compounds are examined, characteristic bands corresponding to -(O···H) vibrations are observed at 3489-3010 cm^{-1}. The changes in these bands were studied through the use of FT-IR spectra because of the interaction of hydrogen bonds of the hydroxyl groups in the ortho, meta and para positions **6a**, **6b** and **6c**, respectively. When the FT-IR spectrum of **6a** is examined, around 3010 cm^{-1} weak bands are observed, indicating that the -OH group in phenyl ring is involved in a strong intramolecular OH···N hydrogen bond. This intramolecular hydrogen bonding occurs between N-H in the benzothiazole ring and -OH group in the phenyl ring. However, in the **6c** compound at the para position, the broad band at 3066 cm^{-1} was observed, which can be attributed to the presence of intermolecular hydrogen bond interactions. The stretching vibrations of the C=N bond in the structure of the benzothiazole ring give medium-intensity peaks in the frequency range of 1602-1587 cm^{-1}. Also, a sharp intense peak observes in the region 1210-1170 and 750 cm^{-1} which belongs to the (C-O) and (C-S) vibrations.

NMR spectral studies

When the ^{1}H-NMR spectra of the ligands are examined, o-hydroxy protons are seen as singlet protons at approximately 12-11 ppm due to the effect of intramolecular hydrogen bonding and phenolic -OH. In addition, p-hydroxy protons were recorded at about 8.02 ppm due to the intermolecular hydrogen bonding effect. Additionally, protons in the structure of the benzothiazole ring are seen as a singlet between 8.13 and 7.98 ppm. In addition, doublet, triplet and multiplet signals between 7.98 and 6.95 ppm correspond to aromatic region protons. In the ^{13}C-NMR spectrum, a downfield shift was observed at 167.8–164.6 ppm due to the presence of the carbon atom double bonded to the nitrogen atoms in the benzothiazole ring. When the spectrum of compounds **6a-c** is examined, the carbon to which the -OH group is attached resonates at 158.2, 158.7 and 160.8 ppm, respectively. It was observed that the carbon signals seen at 158.7-149.5 ppm in phenyl benzothiazoles (**6d-f**) containing two hydroxyl groups belong to the carbons to which the hydroxyl groups in the structure are attached. Other spectral data of the molecule's carbon skeleton fully support the proposed structures. It has been observed in the literature (Khan et al. 2011, Das et al. 2012) that the ^{13}C-NMR spectra of these compounds are quite compatible with these types of compounds.

Thermogravimetric analysis

The thermal stability of the synthesized **6a-f** was examined by TGA-DTA. Thermogravimetric analyzes were performed for the ligand in N_2 atmosphere at a heating rate of 10 °C/min. and using alumina pans. Thanks to the TG curves supported by DTG and DTA studies, the thermal behavior of the ligands was investigated. The TGA results indicated that the thermal decomposition of the synthesized ligands proceeds in one stage. The major decomposition in TG curves (Figure 1) shows the mass losses between 130 and 300 °C for ligands may be attributed to the thermal cleavage of the organic segments. Data on the thermal stability of hydroxy substituted phenyl benzothiazoles (**6a**-**f)** are summarized in Table II.

The melting points (mp) of compounds **6a**-**f** were measured to be 136.6, 132.2, 231.3, 186.2, 143.0 and 223.1 °C, respectively. Compound **6c** showed the highest melting temperature among the six compounds. Due to intramolecular hydrogen bonds are usually stronger than the intermolecular hydrogen bond. Therefore, intermolecular hydrogen bonds provide a stronger driving force for crystallization, showing a higher melting temperature. The results from FT-IR and NMR confirm the presence of the intermolecular hydrogen bond in **6c**. The mp obtained as a result of the DTA analysis are very close to the measured values and those given in the literature data (Khan et al. 2011, Das et al. 2012). The mp of a compound is a measure of its thermal stability. A higher mp indicates a higher resistance to thermal decomposition. Therefore, compounds with higher mp in this ranking are considered to be more thermally stable. Compound **6c** has the highest mp, hence exhibiting the highest thermal stability, followed by compounds **6f, 6d, 6e, 6a,** and **6b** in descending order. The synthesized ligands showed a sharp differential peak in DTG and endothermic peaks associated with loss of organic moiety, corresponding to a major mass loss of about 90%. Finally, TGA/DTA results demonstrated that all ligands were observed to have high decomposition temperatures with high thermal stability; therefore, these compounds can be used as thermally stable materials.

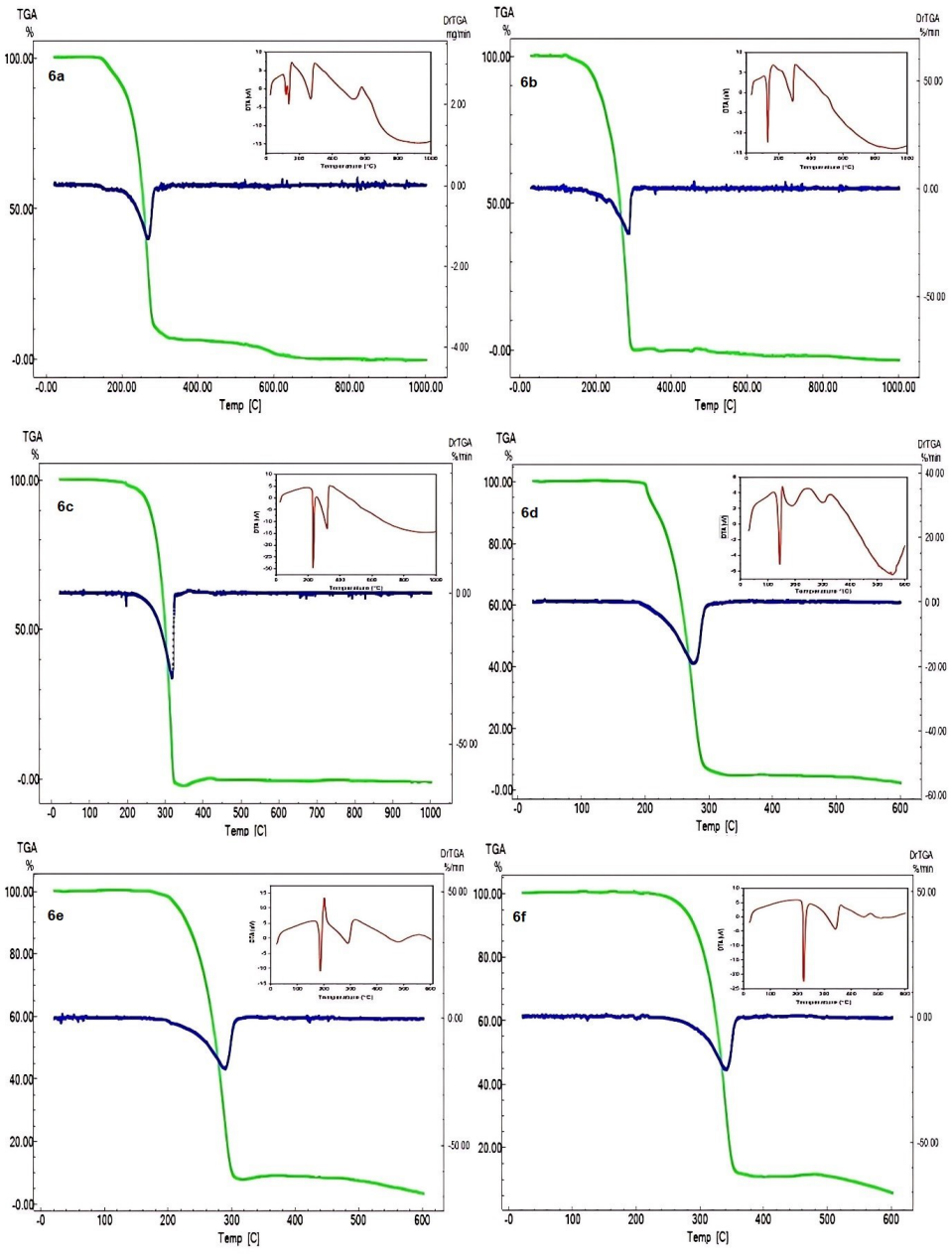

Figure 1. TGA and DTG curves for decomposition of synthesized compounds (inset: DTA curves).

Photophysical properties

The electronic absorption spectrum of **6a-f** was recorded in CH_2Cl_2 at room temperature in the 600-150 nm range. The images of some compounds (**6a, 6d**) under UV light and visible medium are illustrated in Figure 2. The UV-Vis absorption spectrum of **6a-f** exhibits two absorption bands at 238-217 and 321-307 nm, respectively. Figure 2 illustrates the fluorescent emission spectra of compounds **6a-f**. The compound concentration for the analysis was 10^{-6} M and was carried out at room temperature using CH_2Cl_2 solvent. Absorption and emission values of ligands are given in the experimental section. Compounds **6a-6f** showed a Stokes shift between 188-88 nm, although the Stokes shift was found around 50-70 nm in molecules that did not show any difference in their excited

Table II. TGA/DTG/DTA data obtained for 6a-6f ligands.

Compound	Degradation temperature interval (°C)	DTG peak value (°C)	Mass loss (%)	DTA peak value (°C) Endo	Exo	Associated process
6a	140-300	269.4	92.7	118.8 136.6 270.2 -	 581.5	Loss of adsorbed water and/or adsorbed gases Melting point Decomposition of ligands Burning resulting CO_2
6b	130-291	285.6	98.8	132.2 286.9		Melting point Decomposition of ligands
6c	198-321	318.2	99.8	231.3 318.9		Melting point Decomposition of ligands
6d	175-299	290.1	92.7	186.2 288.9 476.4		Melting point Decomposition of ligands
6e	120-310	281.5	93.4	143.0 287.3 -	 551.4	Melting point Decomposition of ligands Burning resulting CO_2
6f	205-350	340.8	88.9 1.2	223.1 340.8 -	 468.4	Melting point Decomposition of ligands Burning resulting CO_2

states (Kaur et al. 2020). In addition, in the emission spectra of the synthesized compounds, it is clearly seen that dual emission occurs in all compounds. The emission spectrum consists of two emission maximums and the values of these maximums vary between 414-301 nm. The shift of the absorption maxima seen in the spectra to longer wavelengths and the slight increase in the molar absorption coefficients are caused by the hydroxy groups in the structure of the ligands (Wang et al. 2018, Kwak & Kim et al. 2009).

When the position of the hydroxy substituents was changed according to the -p, -o and -m position order, it was observed that the emission wavelength was similar, but the fluorescence intensities increased according to the position.

The oxygen atoms of the hydroxy groups in the structure of organic compounds donate electrons to the benzenoid rings and then to the nitrogen atoms in the structure with resonance. This intramolecular hydrogen bond may be one of the reasons for the redshift of the absorption band of the molecules with the longest wavelength, as well as making the molecule harder.

Biological Assessment

Antimicrobial effects of synthesized benzothiazole compounds on bacterial and fungal strains

The antimicrobial activities of the compounds **(6a-6f)** were evaluated against clinically significant bacterial and fungal strains. According to our results, generally, the compounds exhibited significant *in vitro* antimicrobial activity against *Staphylococcus aureus*, *Enterococcus faecalis* (Gram positive bacteria), *Escherichia coli*, *Pseudomonas aeruginosa* (Gram negative bacteria) as well as against *Candida albicans*, *Candida parapsilosis* and *Candida krusei* fungal

strains when compared with commercially antibiotics. Ampicillin and Amikacin were used as standard antibacterial antibiotics. Nystatin was used as standard antifungal antibiotic. The inhibition zones values of all the compounds are shown in Figure 3. The compound **6e** is most active ligand in the series against bacteria and fungi as compared to standard antibiotics. Significantly, compound **6b** containing 3-hydroxy-substituted benzene, unlike the others, showed excellent activity against the *Pseudomonas aeruginosa* (30.00 ± 1.73 mm) strain, moreover, it was more effective than the standard antibiotics used. In addition, compounds **6d** and **6e** having 2,3- and 2,4-dihydroxy substituted benzene ring exhibited superior antibacterial activity against *Staphylococcus aureus* with an inhibition diameter of 34.33 ± 1.15 and 32.00 ± 1.73 mm. The presence of phenolic hydroxyl groups with high protein binding affinity can inhibit microbial enzymes, and also increase the affinity to cytoplasmic membranes, thereby increasing antibacterial activity. Moreover, the increase in the number of hydroxyl groups in

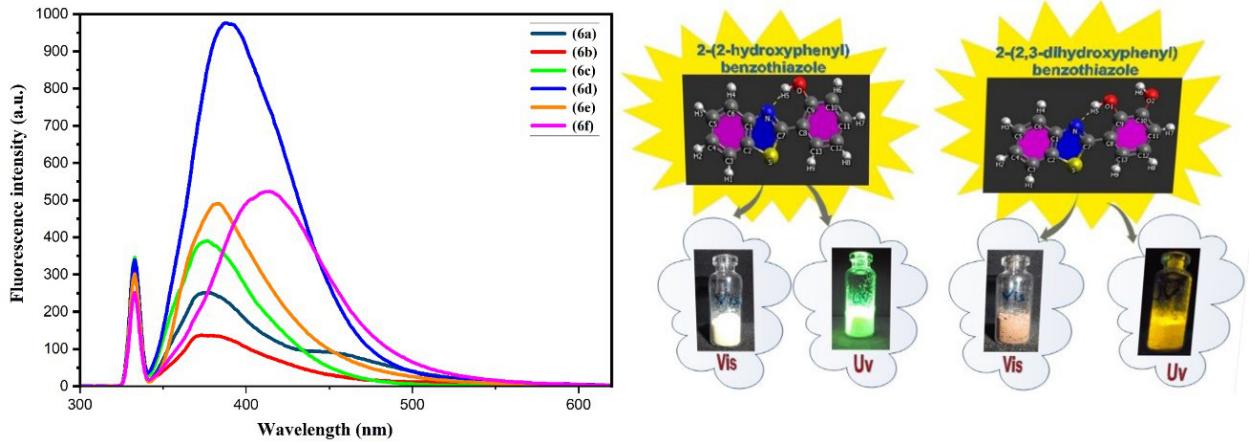

Figure 2. Fluorescence spectra of **6a-f** in CH_2Cl_2 (exc=300 nm for all samples) and the image of some compounds (**6a, 6d**) under UV-light and visible medium.

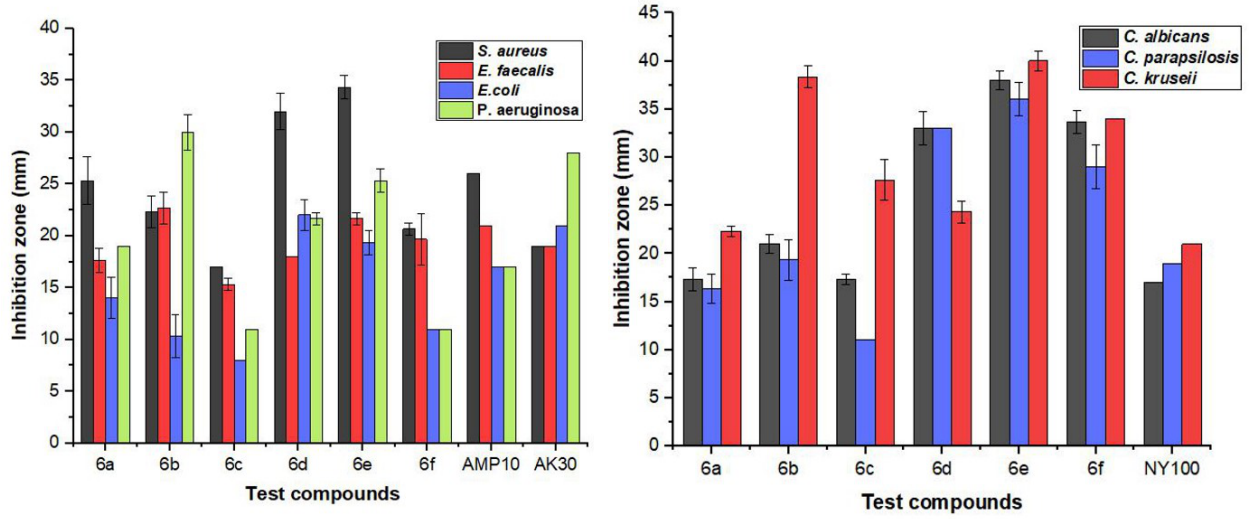

Figure 3. Antimicrobial effects of synthesized benzothiazole compounds.
***Doses of** compounds (6a, 6b, 6c, 6d, 6e, 6f): 30 µg; AM10: Ampicillin 10 µg; AK30: Amikacin 30 µg; NY100: Nystatin 100 µg.

the structure has increased its antibacterial properties regardless of the position in the aromatic structure. According to the results, the compounds (**6d**, **6e** and **6f**) with two hydroxyl groups in their structure exhibit a better level of inhibition activity than other prepared compounds, and their antibacterial activity is higher than compounds **6a**, **6b** and **6c**. The compound 6c, however, exhibited the weakest antimicrobial activity against all strains among all synthesized compounds. According to our results, overall inhibition order is **6e** > **6d** > **6f** > **6b** > **6a** > **6c** as compared to standard antibiotics.

Compounds **6d** and **6b** exhibited excellent antifungal activity against *Candida krusei* yeast with an inhibition diameter of 40.00 ± 1.00 and 38.33 ± 1.15 mm, respectively, when compared to the positive control (21.00 mm). As a result, all tested compounds showed similar or even greater antifungal activity against yeasts than the positive control. In our study, the title compound showed significant inhibition of the tested bacterial and fungal strains, which can be attributed to the presence of electron-donor groups such as hydroxyl in the benzene rings, especially in the 2-position and therefore compounds containing these functional groups showed good activity.

Antiproliferative effects of synthesized benzothiazole compounds on HepG2, HCT116 and AGS cells

Compounds **6a-6f** were administered to HepG2 cells at concentrations of 5-100 µg/mL for 24 hours. While no viability-reducing effect was observed when the compounds were administered at concentrations of 5 and 10 µg/mL, antiproliferative effects were observed at different levels at concentrations of 20 µg/mL and above. Among the compounds applied to HepG2 cells, **6a** and **6d** compounds showed the best antiproliferative effects (IC_{50} value: 13.1 and 31.2 µg/mL, respectively). When **6a** and **6d** compounds were administered at concentration of 40 µg/mL, the viability values were 32 and 48%, respectively. At the highest application concentration of 100 µg/mL, the viability rates for **6a** and **6d** were 19 and 24%, respectively (Figure 4a). The lowest antiproliferative response was observed in HCT116 cells as a result of administration of the compounds. Even at 40 µg/mL application dose, cell viability rates were around 60% except for **6d** and **6f**. Compounds **6d** and **6f** compounds showed a good antiproliferative response in parallel with increasing concentrations (IC50 value: 11.7 and 20.5 µg/mL, respectively). Viability values for **6d** and **6f** at 100 µg/mL application concentration were 24 and 25%, respectively (Figure 4b). Compounds **6a-6f** were applied in AGS cells at concentration of 5-100 µg/mL for 24 hours. There was no proliferation-reducing effect was observed in other compounds, except for compounds **6b** and **6e**, at a concentration of 10 µg/mL. Cell viability percentages were observed as 51 and 54%, respectively, at 10 µg/mL application dose for **6b** and **6e** compounds (IC50 value: 17.2 and 25.6 µg/mL, respectively). In the application of **6b** and **6e** compounds at concentrations of 20 µg/mL and above, cell viability decreased considerably, while this effect was observed for other compounds only at concentration of 100 µg/mL.

Cell viability percentages seen at 10 µg/mL application concentration of **6b** and **6e** compounds were 6 and 3%, respectively (Figure 4c). The best antiproliferative response was observed in AGS cells as a result of administration of the compounds compared to HepG2 and HCT116 cells. Our results clearly demonstrated that the overall antiproliferative effect of the compounds on cells was a concentration-dependent inhibitory effect compared to control cells ($p < 0.05$). This suggests that the

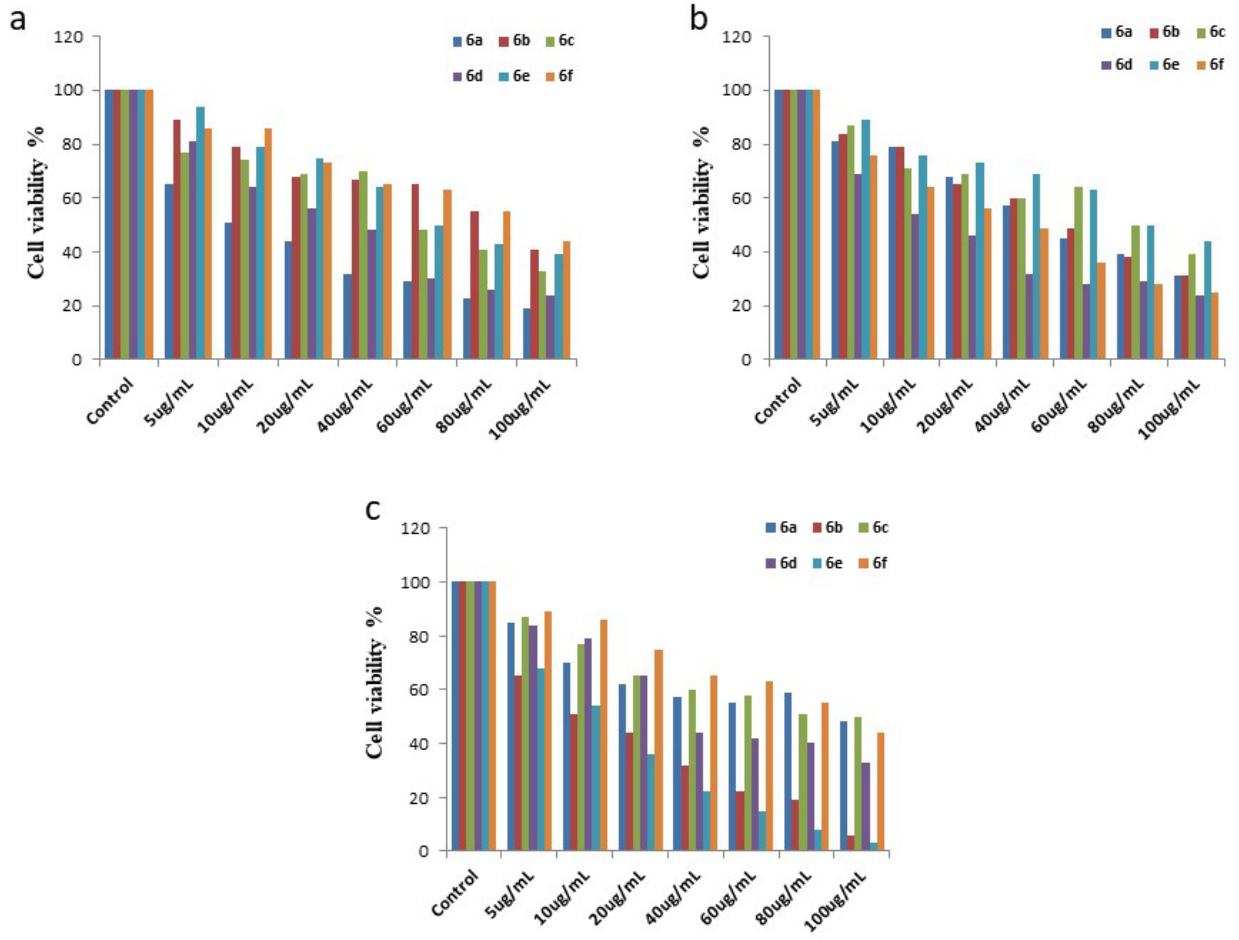

Figure 4. Concentration-dependent antiproliferative effects of synthesized benzothiazole compounds on HepG2 (a), HCT116 (b) and AGS (c) cells.

synthesized benzothiazole compounds may have an important potential in gastrointestinal cancer cells.

Effects of synthesized benzothiazole compounds on Caspase-3, 8 and 9 expressions in HepG2, HCT116 and AGS cells

Among the synthesized benzothiazole compounds, those with the best antiproliferative effects were applied to AGS, HepG2 and HCT116 cells at concentrations of 40 and 100 µg/mL, and the effects of these compounds on caspase-3, 8 and 9 expressions were examined.

The basal caspase expression values of the control group to which the compounds were not administered were naturally different in all three cell lines (Figure 5). After **6b** and **6e** compounds were applied to AGS cells at 40 and 100 µg/mL concentrations, significant increases were observed in the expression of caspase-3, 8 and 9 compared to the control ($p<0.05$). The effects of **6b** and **6e** compounds on caspase-3 activation were close to each other. However, although both compounds increased caspase-8 and 9 activations, clear differences were observed between them. Compounds **6b** induced higher expression of caspase-9, while **6e** highly upregulated caspase-8. In this case, it can be interpreted that **6b** activates the intrinsic pathway of apoptosis in AGS cells, while **6e**

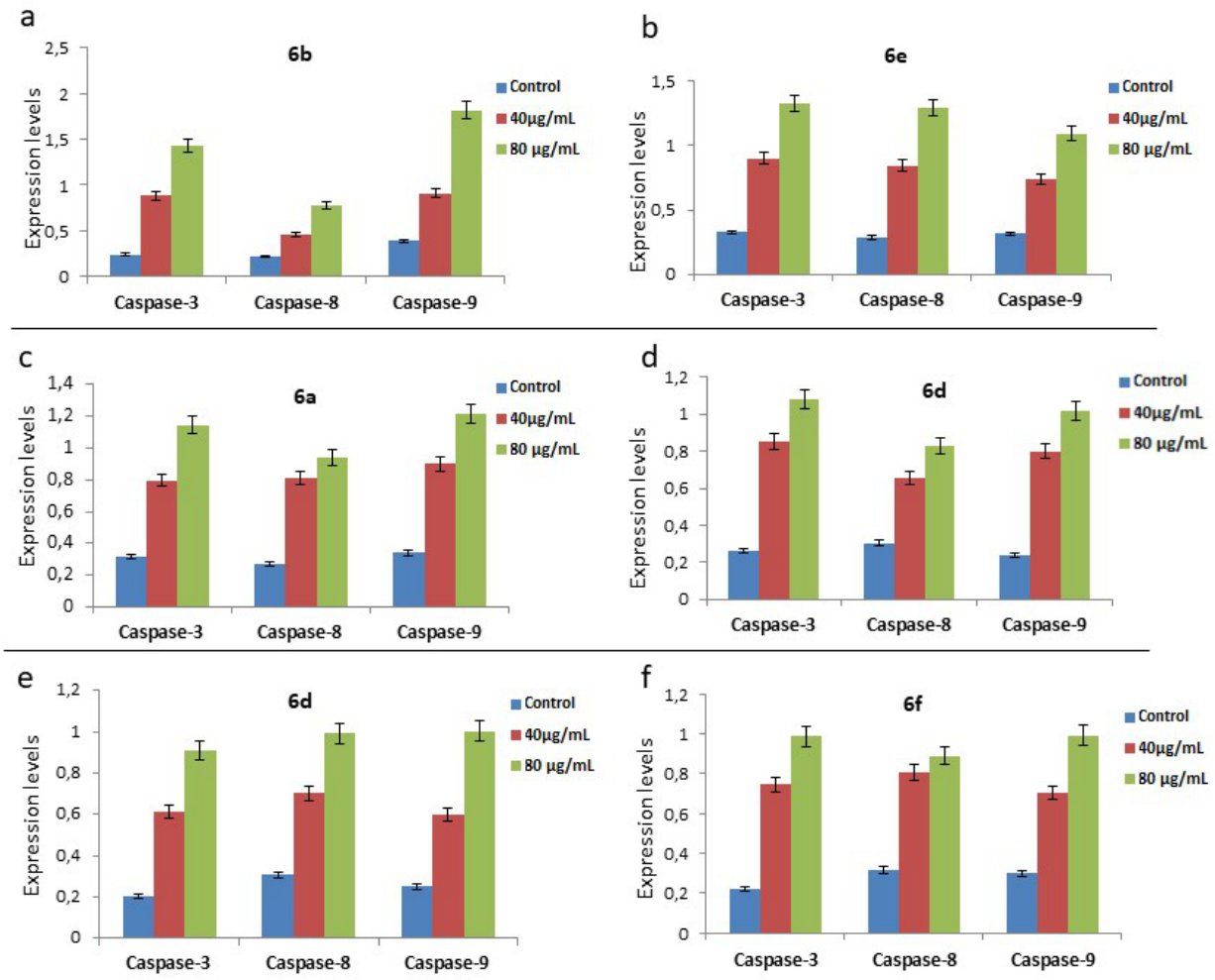

Figure 5. Increased expression effects of caspase-3, 8 and 9 in AGS (a; b), HepG2 (c; d) and HCT116 (e; f) cells after administration of selected benzothiazole compounds with high antiproliferative effect.

activates the extrinsic pathway (Figure 5a, 5b). **6a** and **6d** compounds were administered to HepG2 cells at the same concentrations. Caspase-3, 8 and 9 expressions were significantly increased in HepG2 cells compared to the control group ($p < 0.05$). The increase in caspase-8 and 9 expression was similar for both compounds (Figure 5c, 5d). As a result of the application of **6d** and **6f** compounds to HCT116 cells, significant increases were observed in the expression of caspase-3, 8 and 9 compared to the control ($p < 0.05$). However, unlike other cells, there were no significant differences in caspase-8 and 9 expressions between concentrations (Figure 5e, 5f). However, since the application of benzothiazole compounds in all three cell lines increases caspase activation, which is an important indicator of apoptosis, it can be said that these compounds are potential apoptosis activators.

The effect of synthesized benzothiazole compounds on the migration level in AGS cells

After the application of **6b** and **6e** compounds at a concentration of 80 µg/mL to AGS cells for 24 and 48 hours, the migration changes of the cells were examined with the wound healing assay. As seen in Figure 6, significant effects of **6b** and **6e** compounds on the migration of AGS cells subjected to the scratch assay were observed.

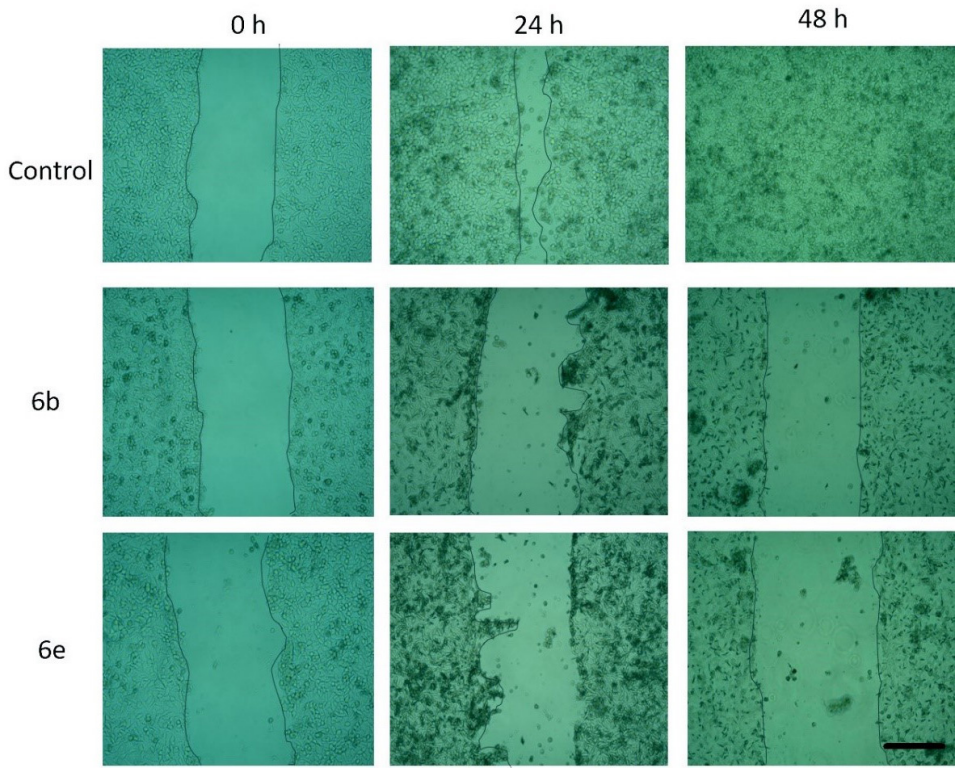

Figure 6. Decreased level of migration in AGS cells after administration of benzothiazole compounds that highly inhibit cell proliferation. Scale bar = 200 µm.

The wound healing rate reached almost complete at the 24th hour in the cell group that did not receive the compound, whereas the wound was completely closed at the 48th hour. After the application of **6b** and **6e** compounds, no change was observed in the wound closure level at the 24th hour compared to the control, but this was the same at the 48th hour, and also significant disruptions in the morphology of the cells were observed (Figure 6).

Kumbhare et al. (2011) reported the synthesis of some arylimidazole derivatives containing the benzothiazole moiety and were screened for their anticancer activity against several cell lines, including HepG2 cells. All these mannich bases benzothiazole scaffolds synthesized showed cytotoxicity at low concentrations against all cell lines tested. In our study, IC50 values of selected compounds were found to be in the range of 11.7-31.2 µg/mL. In a study by Azzam et al. (2022) in which benzothiazole derivatives were applied to cell lines, concentration levels of 70-100 µg/mL were stated to be non-toxic. In the study conducted by Fahim et al. (2022) with another benzothiazole derivatives, IC50 values in HepG2 and HCT116 cells were found to be in the range of 22.5-36.7 µg/mL. One of these compounds also showed specific features of apoptosis as an increase in caspase-3 levels (Kumbhare et al. 2011). Caputo et al. (2012) reported that in their study against various cancer cell lines with an aryl amide and five synthesized derivatives attached to the C-2 of the benzothiazole core, the two compounds showed the best anticancer therapeutic potential due to the presence of electrons, which are the drawing groups in the para position of the phenyl ring. Mortimer et al. (2006) demonstrated the antiproliferative activities of a number of synthesized novel 2-phenyl benzothiazole compounds against lung, colon and breast cancer cells.

Molecular docking studies

The AGS, HCT-116, and HepG2 cancer cell lines are commonly used in research to study various aspects of gastrointestinal cancers, including cancer cell behavior, drug response, and molecular signaling pathways. VEGFR-2, or vascular endothelial growth factor receptor 2, is a protein that plays a critical role in angiogenesis, which is the process of blood vessel formation. VEGFR-2 is often studied in the context of cancer because it is overexpressed in many tumor types and is involved in promoting tumor angiogenesis, which is essential for tumor growth and metastasis (Haider et al. 2021).

In research and drug development, targeting VEGFR-2 has been explored as a potential therapeutic approach for inhibiting angiogenesis and limiting tumor growth in gastrointestinal cancers. There are studies with HepG2 cells to investigate the effects of VEGFR-2 inhibitors or VEGF signaling pathway modulators on processes related to cell proliferation, migration and angiogenesis (Al-Sanea et al. 2023). These studies may help to understand the molecular mechanisms underlying the relationship between VEGFR-2 and tumorigenesis and may contribute to the development of new therapeutic strategies for liver cancer treatment. However, more research is needed to fully elucidate the potential effects of VEGFR-2 on the specific relationship between liver, stomach, and colon cancer biology and treatment.

Molecular docking studies of ligands were performed using 2XIR encoded target VEGFR-2 enzyme. Molecular docking studies were conducted to give clues to the possible mechanism of their cytotoxic effects and to examine ligand-receptor interactions on VEGFR-2 kinase. The binding scores of the **6a** and **6d** ligands for the best binding pose to the 2XIR encoded receptor were found as -8.00 and -9.30 kcal/mol, respectively. In Figure 7a, a hydrogen bond with a distance of 2.20 Å was formed between the hydroxyl group of the **6a** ligand and the ASP1044 key residue (Figure 7b). It was observed that VEGFR-2 formed another hydrogen bond between the essential amino acid LYS868 in its active pocket and the hydroxyl group.

It was observed that the **6d** compound was bonded to the active site of the target by forming two hydrogen bonds to their -OH substitution (Figure 8a, 8b). Especially, the -OH group interacts with the key amino acid, forming the H-bond with the residue Asp1046 and Glu885. Van der Waals, donor-donor, π-cation, π-anion interactions with active site amino acids

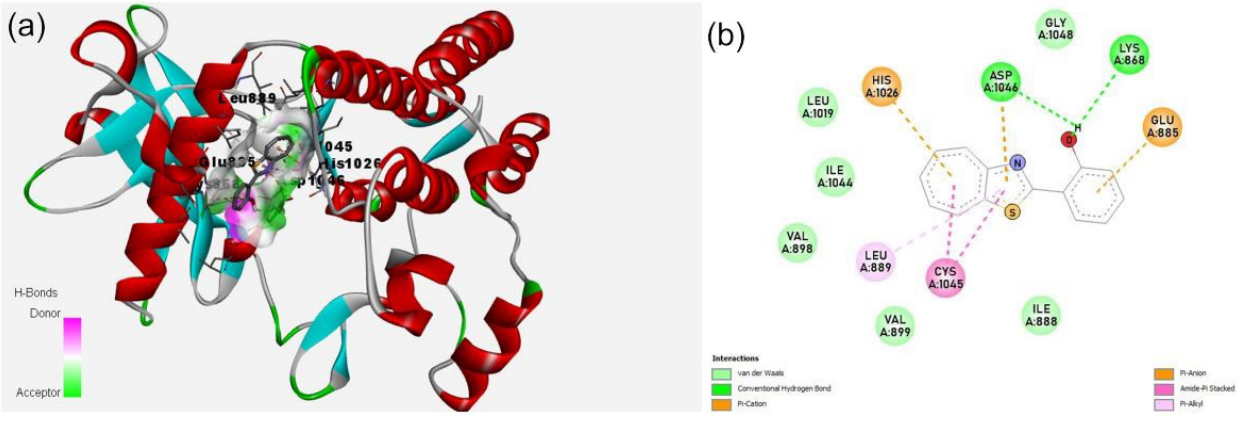

Figure 7. Interactive plot of ligand and receptor and the H-bond surface shown (a), 2D diagram of compound 6a in VEGFR-2 kinase (2XIR) (b).

LYS20, LYS71, ARG192, SER138, ASP282 and LYS288 are other interactions. In addition, amide-π stack interactions were observed between the benzothiazole ring and residues CYS1045.

The docking studies indicated that **6a** and **6d** might be a promising therapeutic agent against cancer infection based on its ability to bind to VEGFR-2 kinase. The above results showed that mentioned compounds emerged as promising as more potential inhibitors of VEGFR-2 kinase.

CONCLUSIONS

In this study, a microwave-assisted protocol for the green synthesis of 2-aryl benzothiazole derivatives **(6a-6f)** was developed. The chemical structure of all the synthesized compounds **(6a-f)** has been confirmed by studying various analytical spectroscopic techniques such as FT-IR, UV-Vis and NMR. TGA/DTA results showed that all ligands have high thermal stability with high decomposition temperature; therefore, these compounds can be used as thermally stable materials. According to the data obtained from TGA analysis, compound **6c** was found to have the highest thermal stability. Furthermore, all synthesized molecules were evaluated for their antimicrobial activity. Compound **6b** containing 3-hydroxy-substituted benzene showed excellent activity against Pseudomonas aeruginosa strain (30.00 ± 1.73 mm), while compounds **6d** and **6e** with 2,3- and 2,4-dihydroxy substituted benzene ring exhibited superior antibacterial activity against Staphylococcus aureus with an inhibition diameter of 34.33 ± 1.15 and 32.00 ± 1.73 mm, respectively, and showed better activity compared to reference molecules. The antiproliferative activity of the synthesized molecules **(6a-6f)** was evaluated against various cell lines including colon, liver and gastric cancer cell lines from the gastrointestinal cancer group and the effects of these compounds on caspase-3, 8 and 9 expressions were studied. The in vitro anticancer results obtained revealed that among the prepared benzothiazole derivatives, some compounds **(6b, 6e)** exhibited good activity against the studied cancer cell lines. Finally, molecular docking studies of the ligands were carried out using the target VEGFR-2 enzyme coded 2XIR. With this work, it offers great potential to design and develop more structurally diverse analogues on the benzothiazole moiety and its derivatives and evaluate them as antitumor agents and design potent VEGFR 2 inhibitors that are more specific and promising as cancer therapeutics.

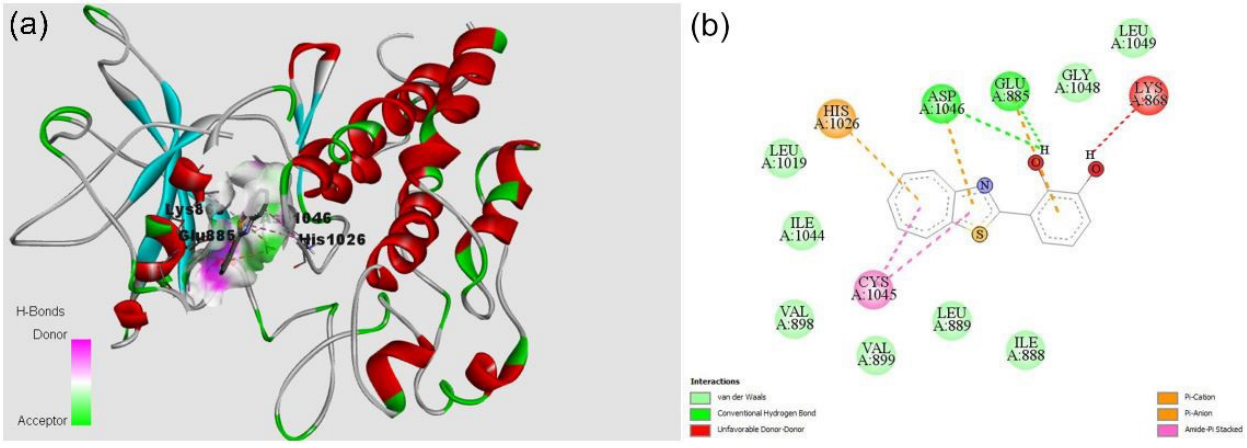

Figure 8. Interactive plot of ligand and receptor and the H-bond surface shown (a), 2D diagram of compound 6d in VEGFR2 kinase (2XIR) (b).

Acknowledgements

This study was financially supported by Duzce University Scientific Research Fund (Project No: 2012.05.HD.051). The authors declare that they have no conflict of interest.

REFERENCES

ABD EL-MEGUID EA, EL-DEEN EMM, MOUSTAFA GO, AWAD HM & NOSSIER ES. 2022. Synthesis, anticancer evaluation and molecular docking of new benzothiazole scaffolds targeting FGFR-1. Bioorg Chem 119: 105504. https://doi.org/10.1016/j.bioorg.2021.105504.

ALLOUCHE A. 2010. Gabedit—a graphical user interface for computational chemistry softwares. J Comput Chem 32: 174-182. https://doi.org/10.1002/jcc.21600.

AL-SANEA MM ET AL. 2023. New benzothiazole hybrids as potential VEGFR-2 inhibitors: design, synthesis, anticancer evaluation, and in silico study. J Enzyme Inhib Med Chem 38(1): 2166036. https://doi.org/10.1080/14756366.2023.2166036.

AMALRAJ SD, PALAPETTA SC & HARICHANDRAN GA. 2022. Facile one-pot synthesis, computational and molecular docking studies of benzimidazole and benzothiazole compounds using Amberlite IRA 400-Cl resin as green/reusable catalyst. J Mol Struc 1268: 133704. https://doi.org/10.1016/j.molstruc.2022.133704.

ANAND P, KUNNUMAKKARA AB, SUNDARAM C, HARIKUMAR KB, THARAKAN ST, LAI OS, SUNG B & AGGARWAL BB. 2008. Cancer is a preventable disease that requires major lifestyle changes. Pharm Res 25(9): 2097-2116. https://doi.org/10.1007/s11095-008-9661-9.

ASADIZADEH S, SOHRABI M, MEREITER K, FARROKHPOUR H, MEGHDADI S & AMIRNASR M. 2022. Novel octanuclear copper (I) clusters $[Cu_8\{(N)\text{-}(_{\mu4}\text{-}S)\}_4(_{\mu3}\text{-}I)_2I_2(PPh_3)_2]$ produced via reductive ss bond cleavage of disulfide schiff base ligands and their use as efficient heterogeneous catalysts in Cuaac click reaction. Mol Catal 524: 112290. https://doi.org/10.1016/j.mcat.2022.112290.

ASLAM B ET AL. 2018. Antibiotic resistance: a rundown of a global crisis. Infect Drug Resist 11: 1645-1658. https://doi.org/10.2147/IDR.S173867.

AZZAM RA, ELGEMEIE GH & OSMAN RR. 2020. Synthesis of novel pyrido[2,1-b]benzothiazole and N-substituted 2-pyridylbenzothiazole derivatives showing remarkable fluorescence and biological activities. J Mol Struct 1201: 127194. https://doi.org/10.1016/j.molstruc.2019.127194.

AZZAM RA, GAD NAGWA M & ELGEMEIE GALAL H. 2022. Novel thiophene thioglycosides substituted with the benzothiazole moiety: synthesis, characterization, antiviral and anticancer evaluations, and NS3/4A and USP7 enzyme inhibitions. ACS Omega 7: 35656- 35667. https://doi.org/10.1021/acsomega.2c03444.

BHOWON MG, JHAUMEER LAULLOO S, HOSTEN EC, ELAHEEBACUS S & DOWLUT MR. 2021. Palladium(II) complexes of (t-butyl salicylidene) diphenyl disulfide diamine: synthesis, structure, spectral characterization and catalytic properties. Transit Met Chem 46(7): 537-545. https://doi.org/10.1007/s11243-021-00471-7.

BOICE A & BOUCHIER-HAYES L. 2020. Targeting apoptotic caspases in cancer. Biochim. Biophys Acta - Mol. Cell Res 1867(6): 118688.

BOUCHET LM, HEREDIA AA, ARGÜELLO JE & SCHMIDT LC. 2020. Riboflavin as photoredox catalyst in the cyclization of thiobenzanilides: synthesis of 2-substituted benzothiazoles. Org Lett 22610-22614. https://doi.org/10.1021/acs.orglett.9b04384.

BRAY F, FERLAY J, SOERJOMATARAM I, SIEGEL RL, TORRE LA & JEMAL A. 2018. Global cancer statistics 2018: globocan estimates of incidence and mortality worldwide for 36 cancers in 185 countries. Cancer J Clin 68: 394-424. https://doi.org/10.3322/caac.21492.

CAPUTO R, CALABRÒ ML, MICALE N, SCHIMMER AD, ALI M, ZAPPALÀ M & GRASSO S. 2012. Synthesis of benzothiazole derivatives and their biological evaluation as anticancer agents. Med Chem Res 21(9): 2644-2651.

CORDEIRO R & KACHROO M. 2020. Synthesis and biological evaluation of anti-tubercular activity of schiff bases of 2-amino thiazoles. Bioorganic Med Chem Lett 30: 127655 https://doi.org/10.1016/j.bmcl.2020.127655.

DALMAZ A, DURMUS S, DÜLGER G & ALPAY M. 2022. Thio-Schiff bases derived from 2,2'-disulfanedianiline via nanocerium oxide: antimicrobial effect and antiproliferative effects in melanoma cells. Turk J Chem 46(4): 1055-1068. https://doi.org/10.55730/1300-0527.3414.

DALMAZ A, DURMUŞ S, DULGER G & DÜLGER B. 2021. Synthesis and characterization of dimeric thio-schiff bases by nano cerium oxide and examination of their antimicrobial activities. Sakarya Univ J Sci 25(2): 364-378. https://doi.org/10.16984/saufenbilder.737671.

DAS A & BANIK BK. 2021. Microwave-assisted synthesis of N-heterocycles, microwaves in chemistry applications. MedChemComm 10: 143-198. https://doi.org/10.1016/b978-0-12-822895-1.00006-0.

DAS S, SAMANTA S, MAJI SK, SAMANTA PK, DUTTA AK, SRIVASTAVA DN, ADHIKARY B & BISWAS P. 2012. Visible-light-driven synthesis of 2-substituted benzothiazoles

using CdS nanosphere as heterogenous recyclable catalyst, Tetrahedron Lett 54(9): 1091-1096. https://doi.org/10.1016/j.tetlet.2012.12.044.

DEBELA DT, MUZAZU SGY, HERARO KD, NDALAMA MT, MESELE BW, HAILE DC, KITUI SK & MANYAZEWAL T. 2021. New approaches and procedures for cancer treatment: Current perspectives. SAGE Open Med 9: 20503121211034366. https://doi.org/10.1177/20503121211034366.

DHADDA S, RAIGAR AK, SAINI K & MANJU GULERIA A. 2021. Benzothiazoles: from recent advances in green synthesis to anti-cancer potential. Sustain Chem Pharm 24: 100521. https://doi.org/10.1016/j.scp.2021.100521.

DHAWALE KD, INGALE AP, SHINDE SV, THORAT NM & PATIL LR. 2021. ZnO-NPs catalyzed condensation of 2-aminothiophenol and aryl/alkyl nitriles: efficient green synthesis of 2-substituted benzothiazoles. Synth Commun 51: 1588-1601. https://doi.org/10.1080/00397911.2021.1894577.

DURMUŞ S, DALMAZ A, DÜLGER G & KADIOĞLU DB. 2017. Synthesis of disulphide-schiff base derivatives and investigations of in vitro antimicrobial activities against some human pathogens. EuroBiotech J 1(3): 230-234. https://doi.org/10.24190/ISSN2564-615X/2017/03.06.

DURMUŞ S, DALMAZ A, ÖZDINÇER M & SIVRIKAYA S. 2017. Preparation of cerium oxide nanoparticles: an efficient catalyst to the synthesis of dimeric disulphide schiff bases. Celal Bayar Univ J Sci 13(1): 25-30. https://doi.org/10.18466/cbujos.282116.

EL-MEGUID EAA, EL-DEEN EMM, MOUSTAFA GO, AWAD HM & NOSSIER ES. 2022. Synthesis, anticancer evaluation and molecular docking of new benzothiazole scaffolds targeting FGFR-1. Bioorg Chem 119: 105504. https://doi.org/10.1016/j.bioorg.2021.105504.

FADDA AA, SOLIMAN NN & BAYOUM NM. 2019. Antimicrobial properties of some new synthesized benzothiazole linked carboxamide, acetohydrazide, and sulfonamide systems. J Heterocyc Chem 56: 2369-2378. https://doi.org/10.1002/jhet.3624.

FLORES-ÁLVAREZ JM, CORTÉS-ARRIAGADA D, GÓMEZ-SANDOVAL Z, JAYAPRAKASH GK, CEBALLOS- MAGAÑA SG & MUÑIZ-VALENCIA PINEDA-URBINA K. 2022. Selective detection of Cu^{2+} ion using a mercaptobenzothiazole disulphide modified carbon paste electrode and bismuth as adjuvant: a theoretical and electrochemical study. New J Chem 46(31): 15052-15063. https://doi.org/10.1039/d2nj02156k.

GAO X, LIU J, ZUO X, FENG X & GAO Y. 2020. Recent advances in synthesis of benzothiazole compounds related to green chemistry. Molecules 25. https://doi.org/10.3390/molecules25071675.

GEDIYA LK & VINCENT CN. 2009. Promise and challenges in drug discovery and development of hybrid anticancer drugs. Expert Opin Drug Discov 4(11): 1099-1110. https://doi.org/10.1517/17460440903341705.

GHANAVATKAR CW, MISHRA VR, SEKAR N, MATHEW E, THOMAS SS & JOE IH. 2019. Benzothiazole pyrazole containing emissive azo dyes decorated with esipt core: linear and non linear optical properties, z scan, optical limiting, laser damage threshold with comparative DFT studies. J Mol Struct 1203: 127401. https://doi.org/10.1016/j.molstruc.2019.127401.

GHANNAM IAY, ABD EL-MEGUID EA, ALI IH, SHEIR DH & EL KERDAWY AM. 2019. Novel 2-arylbenzothiazole dna gyrase inhibitors: synthesis, antimicrobial evaluation, QSAR and molecular docking studies. Bioorg Chem 93: 103373. https://doi.org/10.1016/j.bioorg.2019.103373.

HAIDER K, REHMAN S, PATHAK A, NAJMI AK & YAR MS. 2021. Advances in 2-substituted benzothiazole scaffold-based chemotherapeutic agents. Arch Pharm 1-12. https://doi.org/10.1002/ardp.202100246.

HSU CJ & DING WH. 2022. Determination of benzotriazole and benzothiazole derivatives in tea beverages by deep eutectic solvent-based ultrasound-assisted liquid-phase microextraction and ultrahigh-performance liquid chromatography-high resolution mass spectrometry. Food Chem 368: 130798.

IRFAN A, BATOOL F, NAQVI SAZ, ISLAM A, OSMAN SM, NOCENTINI A, ALISSA SA & SUPURAN CT. 2020. Benzothiazole derivatives as anticancer agents. J Enzyme Inhib Med Chem 35(1): 265-279. https://doi.org/10.1080/14756366.2019.1698036.

KANNAIYAN S, KANNAN K & ANDAL V. 2022. Green synthesis of phenothiazinium schiff base and its nano silver complex using egg white as a catalyst under solvent free condition. Mater Today: Proc 55: 267-273. https://doi.org/10.1016/j.matpr.2021.07.121.

KAUR I, SHIVANI KAUR P & SINGH K. 2020. 2-(2'-Hydroxyphenyl) benzothiazole derivatives: emission and color tuning, Dyes Pigm 176: 108198, https://doi.org/10.1016/j.dyepig.2020.108198.

KAZI I & SEKAR G. 2019. An efficient synthesis of benzothiazole using tetrabromomethane as a halogen bond donor catalyst. Org Biomol Chem 17: 9743-9756. https://doi.org/10.1039/c9ob02125f.

KHAN KM, RAHIM F, HALIM SA, TAHA M, KHAN M, PERVEEN S, HAQ Z, MESAIK MA & CHOUDHARY MI. 2011. Synthesis of novel inhibitors of B-glucuronidase based on benzothiazole skeleton and study of their binding affinity by molecular docking. Bioorg Med Chem19: 4286-4294. https://doi.org/10.1016/j.bmc.2011.05.052.

KUMAR G & SINGH NP. 2021. Synthesis, anti-inflammatory and analgesic evaluation of thiazole/oxazole substituted benzothiazole derivatives. Bioorg Chem 107: 104608.

KUMBHARE MR ET AL. 2011. Synthesis and biological evaluation of novel mannich bases of 2-arylimidazo[2,1-b]benzothiazoles as potential anti-cancer agents. Eur J Med Chem 46: 4258-66.

KWAK MJ & KIM Y. 2009. Photostable BF2-chelated fluorophores based on 2-(2'-Hydroxyphenyl)benzoxazole and 2-(2'-Hydroxyphenyl)benzothiazole. Bull Korean Chem Soc 30(12): 2865. https://doi.org/10.5012/bkcs.2009.30.12.2865.

LUO B, LI D, ZHANG AL & GAO JM. 2018. Synthesis, antifungal activities and molecular docking studies of benzoxazole and benzothiazole derivatives. Molecules 23. https://doi.org/10.3390/molecules23102457.

MAITY S, ROY A, DUARI S, BISWAS S, ELSHARIF AM & BISWAS S. 2021. Brønsted acid mediated nucleophilic functionalization of amides through stable amide c–n bond cleavage; one-step synthesis of 2-substituted benzothiazoles. European J Org Chem 2021: 3569-3572. https://doi.org/10.1002/ejoc.202100645.

MALAH TE, HEGAB MI, AWAD HM, ABDELRAHMAN MT, ABDEL-MEGEID FME, SHAMROUKH AH, ABDEL MAGEID RE & NOUR HF. 2022. Benzothiazole-tethered 1,2,3-triazoles: Synthesis, antimicrobial, antioxidant, and molecular docking studies. J Mol Struc 1266; 133417. https://doi.org/10.1016/j.molstruc.2022.133417.

MARCO-CONTELLES J & SORIANO E. 2011. The medicinal chemistry of hybrid-based drugs targeting multiple sites of action. Curr Top Med Chem 11(22): 2714-2715. https://doi.org/10.2174/156802611798184382.

MATSUNAGA Y, TANG S, MAEDA J, NAKANO Y, PHILIPPE M, SHIBAHARA RJ, LIU MW, SATO H, WANG L & NOLTE RT. 2005. Novel 4-amino-furo[2,3-d]pyrimidines as Tie-2 and VEGFR2 Dual Inhibitors Miyazaki. Bioorg Med Chem Lett 15: 2203-2207.

MOHAMED KS, ELBIALY EE & FADDA AA. 2021. Synthesis of novel heterocycles comprising benzothiazole moiety and their antimicrobial evaluations. Polycycl Aromat Compd 1-14. https://doi.org/10.1080/10406638.2021.1947332.

MORGAN B & MCGILL WJ. 2000. Benzothiazole-accelerated sulfur vulcanization. 2 mercaptobenzothiazole as accelerator for 2,3-dimethyl-2-butene. J Appl Polym Sci 76: 1377-1385. https://doi.org/10.1002/(sici)1097-4628(20000531)76:9<1377::aid app2>3.0.co; 2-a.

MORTIMER CG, WELLS G, CROCHARD JP, STONE EL, BRADSHAW TD, STEVENS MF & WESTWELL AD. 2006. Antitumor Benzothiazoles. 26.(1) 2-(3,4-Dimethoxyphenyl)-5-Fluorobenzothiazole (GW 610, NSC 721648), a simple fluorinated 2-Arylbenzothiazole, shows potent and selective inhibitory activity against lung, colon, and breast cancer cell lines. J Med Chem 49(1): 179-185. https://doi.org/10.1021/jm050942k.

NGUYEN TT, NGUYEN XTT, NGUYEN TLH & TRAN PH. 2019. Synthesis of benzoxazoles, benzimidazoles, and benzothiazoles using a brønsted acidic ionic liquid gel as an efficient heterogeneous catalyst under a solvent-free condition. ACS Omega 4: 368-373. https://doi.org/10.1021/acsomega.8b02932.

OPDENBOSCH NV, LAMKANF M. 2019. Caspases in Cell Death, Inflammation, and Disease. Immunity 50(6): 1352-1364. https://doi.org/10.1016/j.immuni.2019.05.020.

PATEL G, PATEL AR, LAMBAT TL & BANERJEE S. 2021. Direct one-pot synthesis of imines/benzothiazoles/benzoxazoles from nitroarenes via sequential hydrogenationcondensation using nano-$NiFe_2O_4$ as catalyst under microwave irradiation. Curr Res Green Sustain Chem 4: 100149. https://doi.org/10.1016/j.crgsc.2021.100149.

PFEFFER CM & SINGH ATK. 2018. Apoptosis: A target for anticancer therapy. Int J Mol Sci 19(2): 448. https://doi.org/10.3390/ijms19020448.

RACANÉ L, PTIČEK L, FAJDETIĆ G, TRALIĆ-KULENOVIĆ V, KLOBUČAR M, KRALJEVIĆ PAVELIĆ S, PERIĆ M, PALJETAK HČ, VERBANAC D & STARČEVIĆ K. 2020. Green synthesis and biological evaluation of 6-substituted-2-(2-hydroxy/methoxy-phenyl)benzothiazole derivatives as potential antioxidant, antibacterial and antitumor agents. Bioorg Chem 95: 103537. https://doi.org/10.1016/j.bioorg.2019.103537.

RAPOLU T, PAVAN PK, BABU KR, DENDE SK, NIMMAREDDY RR & REDDY LK. 2019. Microwave assisted one pot synthesis of 2-ethylamino benzimidazole, benzoxazole and benzothiazole derivatives. Synth Commun 49: 1308-1315. https://doi.org/10.1080/00397911.2019.1599952.

SEDAGHAT N, NAIMI-JAMAL MR & MOKHTARI J. 2014. Solvent- and catalyst-free synthesis of 2- aryl(heteroaryl)-substituted benzothiazoles. Curr Chem Lett 3: 57-62. https://doi.org/10.5267/j.ccl.2014.2.003.

SHAFI S, MAHBOOB ALAM M, MULAKAYALA N, MULAKAYALA C, VANAJA G, KALLE AM, PALLU R &ALAM MS. 2012. Synthesis of novel 2-mercapto benzothiazole and 1,2,3-triazole based bisheterocycles: their anti-inflammatory and anti-nociceptive activities. Eur J Med Chem 49324-49333. https://doi.org/10.1016/j.ejmech.2012.01.032.

SHAINYAN BA, ZHILITSKAYA LV & YAROSH NO. 2022. Synthetic approaches to biologically active C-2-substituted benzothiazoles. Molecules 27(8): 2598.

SHI WW, SHI C, WANG TY, LI YL, ZHOU YK, ZHANG XH, BIERER D, SHENG JS & LIU L. 2022. Total chemical synthesis of correctly folded disulfide-rich proteins using a removable o-linked β-N-Acetylglucosamine strategy. J Am Chem Soc 144(1): 349-357. https://doi.org/10.1021/jacs.1c10091.

SHIVANI, KAUR I, CHEMMANGHATTU K, KAUR P & SINGH K. 2020. Non-linear optical behavior of benzothiazole based chromophores: second harmonic generation. Dyes Pigm 183: 108739. https://doi.org/10.1016/j.dyepig.2020.108739.

SIRGAMALLA R, KOMMAKULA A, KONDURU S, PONAKANTI R, DEVARAM J & BODA S. 2020. Cupper-catalyzed an efficient synthesis, characterization of 2-substituted benzoxazoles, 2-substituted benzothiazoles derivatives and their anti-fungal activity. Chem Data Collect 27:100362. https://doi.org/10.1016/j.cdc.2020.100362.

SIVRIKAYA S, DALMAZ A & DURMUŞ S. 2018. Synthesis of nano poly (2-thiophenecarboxaldehyde) and characterization of structure. Sakarya University Journal of Science 22(6): 1571-1575. https://doi.org/10.16984/saufenbilder.273829.

STENGER-SMITH J, CHAKRABORTY I, SAMEERA WMC & MASCHARAK PK. 2018. Antimicrobial silver(I) complexes derived from aryl-benzothiazoles as turn-on sensors: synthesis, properties and density functional studies. Inorganica Chim Acta 471: 326-335. https://doi.org/10.1016/j.ica.2017.11.022.

UREMIS N, UREMIS MM, TOLUN FI, CEYLAN M, DOGANER A & KURT AH. 2017. Synthesis of 2-substituted benzothiazole derivatives and their in vitro anticancer effects and antioxidant activities against pancreatic cancer cells. Anticancer Res 37: 6381-6389. https://doi.org/10.21873/anticanres.12091.

WAGAY SA, HASAN A & ALI R. 2022. An efficient low melting mixture mediated green approach for the synthesis of 2-substituted benzothiazoles and benzimidazoles. Results Chem 4: 100338. https://doi.org/10.1016/j.rechem.2022.100338.

WANG L, CUI M, TANG H & CAO D. 2018. Synthesis of a BODIPY-2-(2'-Hydroxyphenyl)benzothiazole conjugate with solid state emission and its application as a fluorescent pH probe. Anal Methods 10: 1633-1639. https://doi.org/10.1039/C8AY00053K.

XU S, LI W, ZUO X, ZHENG D, ZHENG X & ZHANG S. 2016. Structural origin of corrosion inhibition effect over 2-(2-hydroxyphenyl)benzothiazole on steel in HCl medium. Int J Electrochem Sci 14: 5777-5793. https://doi.org/10.20964/2019.06.20.

XU W, JING L, WANG Q, LIN CHUNG-C, CHEN X, DIAO J, LIU Y & SUN X. 2015. Bax-PGAM5LDrp1 complex is required for intrinsic apoptosis execution. Oncotarget 6: 30017-30034. https://doi.org/10.18632/oncotarget.5013.

YAO S, MOYER A, ZHENG Y, SHEN Y, MENG X, YUAN ZHAO Y, YAO H, DAVID B & WU C. 2022. De novo design and directed folding of disulfide-bridged peptide heterodimers. Nat Commun 13(1): 1-10. https://doi.org/10.1038/s41467-022-29210-x.

YU X, ZHANG Z, SONG R, GOU L & WANG G. 2020. Synthesis of 2-aryl-benzothiazoles via Ni catalyzed coupling of benzothiazoles and aryl sulfamates. Heterocycl Commun 26: 1-5. https://doi.org/10.1515/hc-2020-0001.

ZAMAN S, WANG R & GANDHI V. 2014. Targeting the apoptosis pathway in hematologic malignancies. Leuk Lymphoma 55: 1980-1992. https://doi.org/10.3109/10428194.2013.855307.

ZHANG X-Z, ZHOU W-J, YANGA M, WANG J-X & LİN BAİC. 2012. Microwave-assisted synthesis of benzothiazole derivatives using glycerol as green solvent. J Chem Res 36(8):489-491. https://doi.org/ 10.3184/174751912X13400085970187.

How to cite

OZDINCER M, DALMAZ A, DURMUS S, DULGER G & KILICCIOGLU I. 2024. Biological evaluation of benzothiazoles obtained by microwave-green synthesis. An Acad Bras Cienc 96: e20230423. DOI 10.1590/0001-3765202420230423.

Manuscript received on April 11, 2023;
accepted for publication on February 13, 2024

MESUT OZDINCER[1]
https://orcid.org/0000-0002-9378-016X

ASLIHAN DALMAZ[2]
https://orcid.org/0000-0002-1691-2616

SEFA DURMUS[3]
https://orcid.org/0000-0001-6974-513X

GORKEM DULGER[4]
https://orcid.org/0000-0002-1506-1549

ILKER KILICCIOGLU[4]
https://orcid.org/0000-0003-3367-9665

[1]Duzce University, Department of Composite - Materials, Graduate Education Institute, Duzce, 81620, Türkiye

[2]Duzce University, Department of Natural and Herbal Products/Cosmetic Products, Graduate Education Institute, Duzce, 81620, Türkiye

[3]Duzce University, Department of Chemistry, Faculty of Arts and Sciences, Duzce, 81620, Türkiye

[4]Duzce University, Department of Medical Biology, Faculty of Medicine, Duzce, 81620, Türkiye

Correspondence to: **Mesut Ozdincer**
E-mail: mesutozd81@gmail.com

Authors contributions

All authors contributed to the concept and design of the study. MO and AD; designed the experiments, performed the spectroscopic characterization, interpreted the data and performed the experiments. SD and GD contributed to the conceptualization, review and revised the manuscript. IK performed the antiproliferative activity tests and contributed to the evaluation of the results. All authors commented on previous versions of the article. All authors have read and approved the final article.